



Low-fluorinated homopolymer from heterogeneous ATRP of 2,2,2-trifluoroethyl methacrylate mediated by copper complex with nitrogen-based ligand

Guping He^a, Ganwei Zhang^a, Jiwen Hu^{a,*}, Jianping Sun^a, Shenyu Hu^a, Yinhui Li^a, Feng Liu^a, Dingshu Xiao^a, Hailiang Zou^a, Guojun Liu^b

^aGuangzhou Institute of Chemistry, Chinese Academy of Sciences, Guangzhou 510650, PR China

^bDepartment of Chemistry, Queen's University, 90 Bader Lane, Kingston, Ontario, Canada K7L 3N6

ARTICLE INFO

Article history:

Received 8 April 2011

Received in revised form 20 May 2011

Accepted 27 May 2011

Available online 29 June 2011

Keywords:

Nitrogen-based ligand

ATRP

2,2,2-Trifluoroethyl methacrylate

Heterogeneous

ABSTRACT

We report the preparation of low-fluorinated homopolymer via heterogeneous atom transfer radical polymerization (ATRP) of 2,2,2-trifluoroethyl methacrylate (TFEMA) using 2,2'-bipyridine (bpy), *N,N,N',N',N''*-pentamethyldiethylenetriamine (PMDETA), and tris(2-(dimethylamino)ethyl)amine (Me₆TREN) as representatives for di-, tri-, and tetradentate amine ligands, respectively. The ATRP was better controlled, yielding polymers with controlled molecular weights and low polydispersities (M_w/M_n ca. 1.11) when bpy was used as a ligand than when PMDETA was used. This was further supported by the results of our kinetic and chain extension studies. However, the ATRP of TFEMA had lower monomer conversions and gel formation when Me₆TREN was used as the ligand. Further reported are the thermal-properties, as well as the surface properties of the films from the resulting polymers with different molecular weights.

© 2011 Elsevier B.V. All rights reserved.

1. Introduction

Fluorinated (co)polymers, which contain fluorine in their backbones or side chains, have attracted continuous attention from researchers engaged in both fundamental and industrial research [1], since the invention of polytetrafluoroethylene (PTFE) in 1938 [2] and the development of soluble perfluoropolymer (Teflon[®]AF) in 1992 [3]. Indeed, owing to the strong electronegativity and small van der Waals radius (1.32 Å) of fluorine atom, as well as the strong C–F bond (a high dissociation energy of 485 kJ/mol), these kinds of polymers possess unique combined properties. They have good biocompatibility, high thermal stability, good chemical resistance, superior weatherability, oil and water repellence, low flammability, as well as low refractive index, etc. [1,4–7]. Because of these, they have a diverse range of applications in the preparation of many functional materials with notable properties, such as biomaterials, [8] surfactants, [9] lubricants, [10] insulators, [11] ion conducting materials for lithium-ion batteries, [12] proton conducting membranes for fuel cells, paints [13] and coatings [14].

Normally, the incorporation of fluorine into (co)polymers can be accomplished by a variety of synthetic polymerization techniques including cationic polymerization, anionic polymeri-

zation, conventional free radical polymerization, etc. [1]. Among them, conventional free radical polymerization of fluoromonomer, such as fluorinated (meth) acrylates, styrenic and alkenes [15–17], using multiple polymerization processes, e.g. bulk, solution, emulsion, or precipitation polymerization methods [18,19]. An evident drawback of conventional free radical polymerization, however, is that it generates (co)polymers with uncontrolled molecular weights and molecular weight polydispersity (M_w/M_n), as well as ill-defined architecture, because of the very high nonselective activity of the radical, the high termination and transfer of the propagating radical species [18]. To overcome these disadvantages, new techniques are developed based on either reversible deactivation of polymer radicals or a degenerative transfer process, called 'living' or controlled radical polymerization (CRP). The outstanding achievements of CRP methods in the past decade allow for the development of advanced well-defined (co)polymers with various architectures (i.e. telechelic, block, graft, or star copolymers) having predictable molecular weights and low molecular weight polydispersities. As a consequence, the area of self-assembly has also benefited from this, with advances in the preparation of unique structures and many functional materials from self-assembly of copolymers with well-defined structures [20,21].

So far, there have been a number of reports dealing with the preparation of fluorinated or per-fluorinated (co)polymers via controlled/living radical polymerization. Examples include reversible addition-fragmentation chain transfer (RAFT) polymerization,

* Corresponding author. Fax: +86 20 85232307.

E-mail address: hjw@gic.ac.cn (J. Hu).

atom transfer radical polymerization (ATRP), nitroxide-mediated polymerization (NMP), iodine transfer polymerization (ITP), as well as CRP controlled by boron derivatives as activated by oxygen. These controlled radical polymerization techniques have been discussed in detail in a recent book and comprehensive reviews [22]. Among these CRP techniques, ATRP has become one of the most efficient and widely used methods to obtain (co)polymers with different topologies [23,24] since the independently pioneered work by Sawamoto [25a] and Matyjaszewski in 1995 [25b]. In general, this technique comprises a halide functionalized initiator, a transition metal ion (normally, copper(I) ion), and a ligand which forms a complex with the metal ion [25].

Ligands in the ATRP are employed to ensure sufficient solubilization of the transition-metal salt in organic medium and to tune the proper reactivity and dynamic halogen exchange between the metal center and the dormant species or persistent radical [25]. Most of the prior research on ATRP has focused on the nitrogen-based ligands for copper-based ATRP [26], since ligands based on sulfur, oxygen, or phosphorus are often more expensive and less effective due to inappropriate electronic effects or unfavorable binding constants compared to that of nitrogen-based ligands [24a]. So far, two common types of nitrogen ligand developed as active and efficient complexation agents for copper-mediated ATRP [27] are (i) aromatic compounds containing sp²-hybridized nitrogen atoms available in the form of R₁=N–R₂ (such as 2,2'-bipyridine (bpy) and its derivatives) and (ii) aliphatic substances containing sp³ [2] nitrogen atoms in the form of R₁–NR₂–R₃ (such as N,N,N',N',N''-pentamethyldiethylenetriamine (PMDETA) and tris(2-(dimethylamino)ethyl)amine (Me₆TREN) as representatives for tri- and tetradentate amine ligands frequently used for ATRP). Aromatic nitrogen-based ligands usually induce a higher oxidation potential of the complexed metal center, leading to a greater tendency toward radical deactivation in the atom transfer equilibrium and therefore slower overall polymerization rates [28–30]. On the other hand, tridentate and tetradentate aliphatic amine ligands generally provide faster polymerizations without causing significant broadening of the molecular weight distribution of the product [28]. In other words, the use of an appropriate ligand is still of major importance to provide an efficient halogen-exchange reaction between the dormant and the active species in the ATRP as well as to produce polymers with controlled molecular weights and low polydispersities [31].

2,2,2-Trifluoroethyl methacrylate (TFEMA), a commercially available monomer with a low level of fluorination, generates the (co)polymers with combined features as those from typical methacrylate monomers and fluorine-containing monomer simultaneously [32]. Therefore, the (co)polymers derived from TFEMA can be utilized for the fabrication of many functional materials. For example, they can be used in coatings, resin modification, and adhesives because of their non-cohesiveness as well as water and oil repellency [33–35]. They are utilized in contact lenses because of enhanced oxygen permeability in a fluorinated matrix [36]. Furthermore, their electron-withdrawing properties have facilitated their use as an electrical charge control agent in photocopy toners [37], and their superior mechanical strength and low refractive index have facilitated their use in optical fiber [38]. Also, the fluorine electronic effect is taken advantage of in ¹⁹F MRI imaging applications [39].

The controlled polymerization of TFEMA could be dated to 2001, in which Roussel and Boutevin reported the controlled polymerization of TFEMA by the “iniferter (initiation-transfer-termination)” method using a substituted fluorinated tetraphenylethane-type initiator [40]. More recently, RAFT (co)polymerizations involving TFEMA were reported. For example, PTFEMA was grafted onto ramie fibers in supercritical carbon

dioxide [41], and butyl methacrylate and TFEMA were copolymerized via RAFT miniemulsion polymerization [42]. To date, there have also been a few reports on the ATRP of TFEMA [3–47]. For example, Perrier reported the synthesis of PTFEMA with average polymerization degrees less than 100 at 90 °C. 2-ethyl bromoisobutyrate and Cu(I)Br/N-(*n*-pentyl)-2-pyridylmethanimine in toluene were used as the initiating system. The resultant polymers had relatively low polydispersity at all stages of polymerization (PDI ~ 1.30). They further demonstrated the poor initiator efficiency and a gradual loss of reactive species resulting from irreversible termination during polymerization [43]. Hvilsted and his coworkers reported the controlled ATRP of TFEMA initiated with 2-ethylbromoisobutyrate (2EBiB) and Cu(I)Br/N-(*n*-propyl)-2-pyridylmethanimine to synthesize amphiphilic block copolymers of TFEMA and MMA, 2-methoxyethyl acrylate, or poly(ethylene oxide) methyl ether methacrylate [44]. Zhu and coworkers reported the preparation and aggregating behavior of a ABCBA-type pentablock copolymer, PDMAEMA-*b*-PTFEMA-*b*-PCL-*b*-PTFEMA-*b*-PDMAEMA via consecutive ATRP using poly(ε-caprolactone), Br–PCL–Br, as the initiating block to polymerize TFEMA in the presence of CuCl/bpy in DMF at 85 °C [45]. A series of well-defined diblock copolymers of acrylic acid with partially fluorinated acrylate (TFEMA) and methacrylate monomers were synthesized using ATRP to serve as potential ¹⁹F MRI imaging agents by Whittaker and colleague. They declared that poly(*tert*-butyl acrylate)-*b*-poly[butyl acrylate-*co*-FEMA] (ptBA-*b*-p(BA-*co*-FEMA)) copolymers were initiated from macroinitiator, PtBA–Br, at 90 °C in toluene using CuBr/PMDETA as catalytic system, and the conversion limited to 40% for the second block [46]. Wooley and her coworkers also prepared amphiphilic hyperbranched partially fluorinated copolymers for the potential application as ¹⁹F MRI imaging agents [47]. The work on ATRP of TFEMA reported, so far, indicates either lower monomer conversion or loss of control, therefore, it is worthy to carry a systematically study on ATRP of TFEMA.

1.1. TFEMA ATRP

When one of the oxidation states of the metal–ligand complex is less soluble, a heterogeneous system can originate, which can result in complex polymerization kinetics and even loss of polymerization control. This can be usually found in systems with bpy [48,49] and multi-dentate aliphatic amine ligands [50]. However, these disadvantages are accompanied by some major advantages, namely the ligands are cheap, easily accessible (especially the multi-dentate amines), and easily separated from the polymer solution because of the heterogeneity of the metal/ligand complexes [51]. In the present contribution, in an effort to have better control on TFEMA ATRP, we study the heterogeneous ATRP of TFEMA using bpy, PMDETA, and Me₆TREN as representatives for di-, tri-, and tetradentate amine ligands, respectively (Fig. 1). The properties of the resulting homopolymers, PTFEMA, with various molecular weights are also investigated.

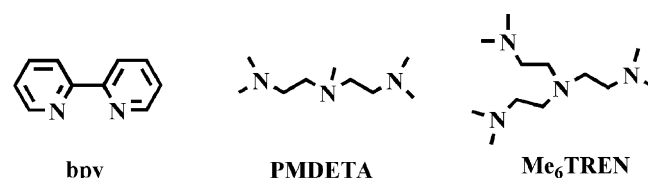


Fig. 1. Ligands used for ATRP of TFEMA.

2. Experimental

2.1. Materials and reagents

TFEMA, purchased from Harbin Xeogia Fluorine-Silicone Chemical Company, China, was washed with 2 wt.% aqueous solution of sodium hydroxide, and then with double-distilled water several times till neutralization. The organic layer was collected and dried over anhydrous magnesium sulfate before distillation under reduced pressure just before use. Copper(I) bromide (CuBr, Fluka, 99+%) was purified by stirring in glacial acetic acid at 80 °C for over 8 h, followed by washing with dry methanol over 10 times before drying in vacuum at room temperature for 48 h, according to the method reported in our previous paper [52]. Copper(I) chloride (CuCl, Aldrich, 99%) was purified using a method similar to that used for CuBr. *N,N,N',N',N'*-pentamethyldiethylenetriamine (PMDETA, Aldrich, 99+%) and 2,2'-bipyridine (bpy) (Aldrich, 99%) were used as received. Cyclohexanone purchased from Tianjin Baishi Chemical (99.8%) was initially decolorized by active carbon, and then stirred with calcium hydride (Aldrich, 99%) overnight before distillation under reduced pressure prior to use. Tetrahydrofuran (THF), diethyl ether, acetonitrile and hexane were all of analytical grade and distilled over sodium wires prior to use. Hydroxyethyl methacrylate (HEMA) was purified using the following procedures: washing the aqueous solution of HEMA (100 mL HEMA and 300 mL deionized water) with hexanes for eight times (8 × 50 mL), after removing the organic layer, salting HEMA out from the aqueous phase by addition of NaCl, drying over anhydrous magnesium sulfate, and finally distilling under reduced pressure. Trimethylsiloxyethyl methacrylate (HEMA-tms) was prepared and purified according to a literature procedure [53]. Other reagents, if not specified, were treated using normal procedures that were used in the lab.

2.2. Preparation of methoxyl ethylene 2-bromoisobutyrate (MEBrIB)

MEBrIB was synthesized by reacting anhydrous ethylene glycol monomethyl ether with 1.2 equivalent of 2-bromoisobutryl bromide in dry diethyl ether in the presence of triethylamine as acid absorbent at room temperature overnight. After removing triethylamine hydrogen bromide salt by centrifugation, the reaction mixture was successively washed with 2 N HCl, saturated sodium carbonate, and double distilled water before drying over anhydrous magnesium sulfate. The crude product was isolated as a slight colorless liquid upon removal of the solvent and purified by distillation under vacuum (~1 mmHg) at 74–76 °C at a yield of 90%. ¹H NMR (CDCl₃, 400 MHz): δ 4.3 (t, 2H), δ 3.6 (t, 2H), 3.37 (s, 3H); δ 1.93 (s, 6H).

2.3. Preparation of tris(2-(dimethylamino)ethyl)amine (Me₆TREN)

Me₆TREN was prepared as we previously reported [52]. Briefly, to prepare the salt (CINH₃CH₂CH₂)₃NHCl, 30 mL of 3.0 M HCl in methanol was added dropwise to 4.0 mL or 0.027 mol of tris(2-aminoethyl)amine in 50 mL of methanol. After stirring at room temperature for 1 h, the precipitate was filtered and washed with 50 mL of methanol thrice to yield 6.72 g or 0.026 mol of product in 98% yield. Then, 6.72 g of (CINH₃CH₂CH₂)₃NHCl, 10 mL of distilled water, 50 mL of formic acid, and 46 mL of a formaldehyde aqueous solution were mixed. The mixture was heated under stirring in a 120 °C oil bath for 6 h before volatile components were removed by rotary-evaporation. To the solid residue was then added 100 mL of 10 wt.% NaOH aqueous solution. The resulting aqueous phase was extracted with 100 mL of diethyl ether for four times. The organic layer was collected, dried over anhydrous NaOH, and concentrated by rotary evaporation. After vacuum distillation at 62 °C, 6.0 g of

the product was obtained as colorless oil at a yield of 89%. ¹H NMR (CDCl₃, 400 MHz): δ 2.20 (s, 18H, CH₃); δ 2.3–2.37 (m, 6H, CH₂); δ 2.56–2.60 (m, 6H, CH₂).

2.4. Characterization

¹H NMR spectroscopy measurements were recorded on a Bruker DMX-400 spectrometer with a Varian probe in deuterated chloroform. The concentration of sample in CDCl₃ typically used for ¹H NMR measurement was about 5–10 mg/mL. *Size exclusive chromatography (SEC)* was performed using a Waters 1515 series GPC system equipped with a Waters 2414 refractive index (RI) detector and a set column of styragel HR4 and HR3 at 35 °C. The correlation between the elution time and the polymer molecular weight was predetermined by low-polydisperse polystyrene standards. The samples usually at a concentration of 5–10 mg/mL in DMF were filtrated through 0.45 μm before injection. The mobile phase was HPLC grade DMF at a speed of 0.6 mL/min. *FT-IR spectra* were recorded using a Bruker FT-VERTEX 70 at a scan range of 400–4000 cm⁻¹ with an accuracy of 2 cm⁻¹. Sample for testing was initially mixed with KBr and pressed to a circular sheet before FTIR evaluation. *The glass transition temperatures (T_g)* were determined with a DSC Q200 system (TA Co. Ltd., USA). Sample was heated from room temperature to 150 °C at a rate of 10 °C/min and kept for 3 min before cooled to -50 °C at a rate of 10 °C/min to remove any effects induced by prior treatments. The T_g was then determined by consecutive heating from -50 °C to 200 °C at a rate 10 °C/min. *Thermogravimetric analysis (TGA)* was performed on a thermoanalyzer system (model Q600SDT, TA Co. Ltd., USA) by heating 5–8 mg of sample from room temperature to 500 °C at a rate of 20 °C/min under nitrogen atmosphere. The onset temperature, decomposition temperature and residual mass were calculated with the TA Instruments Universal Analysis 2000 software. All samples were vacuum dried at 50 °C for 24 h prior to measurements. *Contact angle* measurements were estimated on an OCA40 plus contact angle system apparatus from Dataphysics with contact angles attained by the drop-shape (geometry) method [54]. Films for contact angle measurements were prepared at room temperature under dry atmosphere in a desiccator by dropping a few drops of polymer solution in THF at 0.2 g/mL onto glass slide, which was initially cleaned in sequence with methanol, acetone, and deionized water. A drop of testing liquid (5 μL, pure water or CH₂I₂) was placed via syringe onto the resulting polymer film and the image was immediately sent via the CCD camera to the computer for analysis. Contact angle was reported as averaged at least ten different positions for the same film.

2.5. General procedures for ATRP of TFEMA

The ATRP of TFEMA was performed in cyclohexanone using CuBr as a catalyst in the presence of different ligands. In a typical run, cyclohexanone (6 mL), TFEMA (5.011 g, 29.76 mmol), MEBrIB (50.3 mg, 0.2237 mmol), and bpy (69.8 mg, 0.4475 mmol) were added in one of the flasks of a home-made two-flask set connecting two 25 mL flasks via a glass pipe with a diameter of 0.8 cm and length of 5 cm, while CuBr (32.1 mg, 0.2237 mmol) was loaded to the other flask. The liquid mixture was bubbled with pure argon for over half an hour before subjected to three freeze-pump-thaw cycles, and then, carefully transferred to the flask containing CuBr and put into an oil-bath with a constant temperature of 80 °C. The reaction was stopped by freezing the flask with liquid nitrogen before exposure to air as indicated by color of the solution turning from pale green to blue within 1 min. Then, the blue reaction mixture was diluted with 5 mL of THF before passing through a neutral alumina column to remove copper complex. The filtrate was concentrated to about 10 mL with rotary-evaporation before

precipitated out over 100 mL of hexane. The crude product was purified by repeatedly dissolving in 5 mL of THF and precipitated out over 100 mL of hexane twice before dried overnight under vacuum to generate 3.8 g of polymer as white powder. ^1H NMR (CDCl_3): δ 4.32 (br s, $-\text{CH}_2\text{CF}_3$); δ 3.35 (br s, $-\text{OCH}_3$); δ 1.75–2.05 (m, $-\text{CH}_2$); δ 0.75–1.35 (m, $-\text{CH}_3$); $M_w/M_n = 1.11$.

2.6. Kinetic study of ATRP of TFEMA

To monitor the ATRP kinetic, in situ ^1H NMR spectra were collected with different time intervals. In a representative run, cyclohexanone (5 mL), TFEMA (5.0310 g, 29.8 mmol), MEBriB (66.9 mg, 0.298 mmol), and bpy (92.8 mg, 0.595 mmol) were added to one flask of a two-connective flask set and CuBr (42.7 mg, 0.298 mmol) was added to the other flask of the connective flask. The reactants were bubbled for half an hour with argon before subjected to three freeze pump thaw cycles and then transferred the liquid reactants to the flask containing CuBr. The solution was put into an oil-bath preheated to 80 °C with constant stirring. Samples were withdrawn with time intervals in order to investigate the nature of the TFEMA polymerization by ^1H NMR and SEC analyses. Conversion and SEC analysis were directly performed for the withdrawn samples. Conversions were estimated from ^1H NMR analysis by comparison of sum of the peak intensity for the double bond $-\text{CH}_d\text{CH}_2$ (5.85 and 6.19 ppm) protons from TFEMA to the sum of that for $-\text{CH}_2-\text{CF}_3$ from fluorinated methacrylate at δ 4.49 ppm (monomer) and δ 4.33 ppm (polymer). For molecular weight evaluation, the withdrawn sample was concentrated with nitrogen flow, then added hexane to set out down all the polymer and then dried under vacuum for 48 h before ^1H NMR analysis. The ^1H NMR results for the evaluation of molecular weight employed in the kinetic curve only consist of samples more than 30% conversion based on after precipitation.

2.7. Chain extension using PTFEMA as macroinitiator

In a representative run, acetonitrile (0.7 mL), HEMA-tms (0.3011 g, 1.47 mmol) and bpy (11.5 mg, 0.0739 mmol) were added in one flask of a two-connective flask set, while PTFEMA (0.4172 g, or 0.0369 mmol, DP = 66 as evaluated from ^1H NMR, and $M_w/M_n = 1.24$), and CuCl (3.7 mg, 0.0369 mmol) were added to the other flask. The reactants were bubbled for half an hour with argon before subjected to three freeze–pump–thaw cycles, and then transferred the liquid reactants to the flask containing solid reactants. The brownish red solution was stirred and put into an oil-bath preheated to 70 °C. The reaction was also stopped by freezing with liquid nitrogen before exposure with air, and then, precipitated out over ice. The precipitation was washed with 100 mL of hexane for 3 times before vacuum drying for 48 h, generating 0.6842 g (monomer conversion = 89%) of product as white powder. $M_w/M_n = 1.27$. ^1H NMR ($\text{DMSO}-d_6$): δ 4.33 (br s, 2nH, $-\text{CH}_2\text{CF}_3$); δ 3.95 (br s, 2mH, $-\text{COOCH}_2-$ in the PHEMA-tms chains); δ 3.75 (br s, 2mH, $-\text{CH}_2\text{OSi}$); δ 1.7–2.1 (br, 2(n + m)H, $-\text{CH}_2-$ in the main chain); δ 0.8–1.3 (br, 3(n + m)H, $-\text{CH}_3$ in the main chain); δ 0.1 (br s, 9mH, $-\text{Si}(\text{CH}_3)_3$).

3. Results and discussion

3.1. ATRP of TFEMA using PMDETA as ligand

At the initial stage of this work, we roughly examined the ATRP of TFEMA using MEBriB as an initiator in the presence of CuBr as a catalyst and PMDETA as a ligand in cyclohexanone at 70 °C. To prepare objective homopolymer PTFEMA with the theoretical maximum repeating units of 400, the $[\text{M}]_0/[\text{I}]_0/[\text{L}]_0$ was set at 400/1/1, while solvent/monomer (S/M , v/v) was set at 1.3/1. Here $[\text{M}]_0$, $[\text{I}]_0$, and

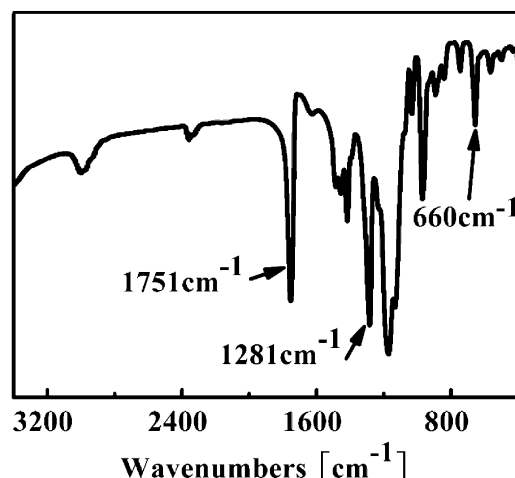


Fig. 2. FT-IR spectrum of homopolymer PTFEMA.

$[\text{L}]_0$ represent the initial concentration of monomer, initiator, and ligand, respectively. The reaction mixture turned from yellow to green right away, and then the whole reaction mixture successively becomes dark green and opaque. The viscosity of the reaction mixture progressively increased after 1 h indicating polymerization [55]. After stopping the reaction by freezing the reaction mixture with liquid nitrogen and introducing the air to the reaction mixture, the green color of the mixture immediately turned blue demonstrating that all the Cu(I) complex transferred to Cu(II) complex [55]. The yield of the product as white powder was about 69% after purification as judged by gravimetric method. Fig. 2 shows the FT-IR spectrum of homopolymer PTFEMA from ATRP. The characteristic band at 1751 cm^{-1} corresponds to ester carbonyl ($\text{C}=\text{O}$) bonds, and the peaks at 660 cm^{-1} and 1281 cm^{-1} are attributed to the stretching and bending vibration of $\text{C}-\text{F}$ bonds, respectively [41]. The disappearance of absorption peak at 1640 cm^{-1} from stretching vibration of $\text{C}=\text{C}$ bond in the monomer TFEMA indicates successful polymerization of TFEMA [56].

Fig. 3 shows ^1H NMR spectrum and peak assignments of initiator, monomer, and PTFEMA, respectively. The changes in the chemical shift of CH_2 (vinyl group in the monomer) protons from 6.20 and 5.67 ppm to 2.17 ppm (backbone in the polymer) indicate the polymerization of monomer. The chemical shift belongs to protons of methylene groups attached to $-\text{CF}_3$ moved from 4.51 ppm to 4.32 ppm after the polymerization of TFEMA because of the weakened $p-\pi$ conjugation effect [56]. Also, the resonance for $-\text{OCH}_3$, normally at ~ 3.7 ppm in poly(methyl methacrylate), shifts to 4.31 ppm in PTFEMA due to the strong electron withdrawing effect from $-\text{CF}_3$ group in PTFEMA [57].

The monofunctional initiator MEBriB was extensively employed for ATRP in our lab as a probe for ^1H NMR analysis to facilely assess the true molecular weight due to the resonance of protons ($-\text{OCH}_2\text{CH}_2\text{OCH}_3$) incorporated into the polymer chain end located in a clear region of the spectrum [58]. However, this is only possible for relatively low molecular weights ($M_n < 15,000$ g/mol). Otherwise the signal of this group becomes negligible in comparison with the signals of the other protons in the polymer chain. Here, the average polymerization degree (DP) can be readily calculated by comparing the peak intensity integration (S) of 3.35 ppm from $-\text{OCH}_3$ (o) at the end of the polymer chain introduced by initiator to that of 4.32 ppm from $-\text{CH}_2\text{CF}_3$ (m) at the repeating unit of polymer chain with Eq. (1).

$$\text{DP} = \frac{3S_m}{2S_o} \quad (1)$$

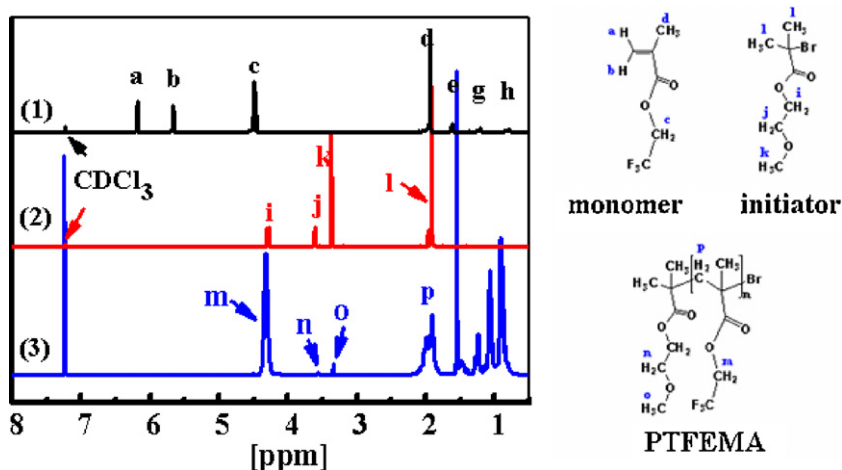


Fig. 3. ^1H NMR spectra of (1) monomer, (2) initiator, and (3) PTFEMA recorded in CDCl_3 at 30°C .

The SEC results demonstrate that the number average molecular weight (M_n) of the resulting polymer is 100,450 g/mol ($\text{DP} = 598$) and molecular polydispersity (M_w/M_n) is 1.52 using PS as standard, whereas the number average molecular weight (M_n) of the resulting polymer as evaluated from ^1H NMR with Eq. (1) is 64,170 g/mol ($\text{DP} = 382$), the difference of M_n from SEC to that from NMR is ascribed from difference of the hydrodynamic volume of PTFEMA to that of PS used for calibrating the SEC columns [52]. Moreover, the DP from gravimetric method (monomer conversion $\sim 69\%$, here, the DP from conversion is based on the assuming that an ideal living polymerization occurred) is around 296, and that from ^1H NMR is 382. This difference suggests that irreversible termination, or low initiation efficiency, or loss of active specie possibly occurred during the polymerization [22,23]. Careful inspection of the broad but monomodal SEC profile of this sample prepared using PMDETA as a ligand reveals no obvious evidence of permanent termination from recombination in the initial and final stages of the polymerization, since no high molecular weight tails and low molecular weight shoulders could be observed (Fig. 4).

3.2. ATRP with various commonly used ligands

To investigate the details for ATRP of TFEMA with predesigned average polymerization degree (DP) using PMDETA as ligand, we then performed ATRP of TFEMA by varying $[\text{M}]_0/[\text{I}]_0$, polymerization time, or S/M (v/v). The reaction recipe, monomer conversion,

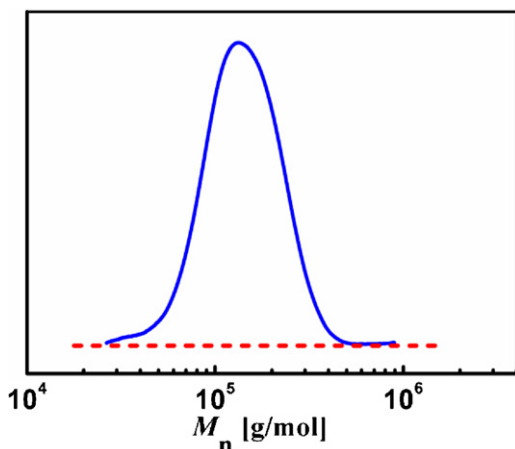


Fig. 4. SEC curve of PTFEMA prepared using PMDETA as ligand.

molecular weight and its polydispersity are summarized and listed in Table 1 (entries 1–4).

It clearly shows that the conversion increased with the increase of the reaction time regardless of the ratio of $[\text{M}]_0/[\text{I}]_0$. For example, a conversion of 56% was achieved after 4 h (entry 3 in Table 1) compared to that of 81% (entry 3) after 6.5 h when $[\text{M}]_0/[\text{I}]_0/[\text{L}]$ was set to 135/1/1, while a conversion of 74% was obtained after 5.5 h (entry 2) compared to that of 80% (entry 4) after 6 h when $[\text{M}]_0/[\text{I}]_0/[\text{L}]$ was set to 270/1/1. However, the molecular weight as evaluated based on conversion from ^1H NMR is lower than that from Eq. (1), suggesting the possible loss of the active end group or irreversible termination during the chain propagation. Moreover, the molecular weight polydispersity index (M_w/M_n) of the resulting polymer samples is relatively higher, for example, ranging from 1.4 to 1.54, especially when preparing the polymer with high targeting polymerization degree and high conversion. This indicates that TFEMA ATRP using PMDETA as the ligand was not well controlled.

To have better control on the preparation of PTFEMA, we thus investigated the effect of other ligand, bpy, on ATRP of TFEMA in terms of conversion, molecular weight and its polydispersity. The results are also summarized and listed in Table 1 (entries 5–10). The homopolymers with different molecular weights were successfully synthesized with bpy as ligand judging by low molecular weight polydispersity index (M_w/M_n , 1.11–1.29) for the resulting polymer at high monomer conversion and high targeted DP. In addition, a narrow PDI (M_w/M_n) was obtained when $[\text{CuBr}]/[\text{bpy}]$ was set to 1/2 compared to a broader one to that set to 1/1 (entries 6–9), which is consistent with the observation from others when preparing polystyrene (PS) and poly(methyl acrylate) with an optimum ligand-to-copper(I) halide ratio of 2/1 [56]. Moreover, when a higher molecular weight was targeted by setting $[\text{M}]_0/[\text{I}]_0/[\text{L}]$ to 400/1/2 (entries 9 and 10), a relatively broader PDI and lower monomer conversion were achieved compared to that with a lower targeting molecular weight, which can be explained by the fact that termination and other side reactions are also presented in ATRP, and they become more prominent as higher molecular weight polymers are targeted [60].

As stated early, Me_6TREN is commonly employed as representative tetradentate amine ligand in the ATRP of many monomers [28]. In our system, as shown in entries 11–16 in Table 1, each polymerization had a monomer conversion less than 30% when Me_6TREN was used as a ligand. While Me_6TREN was employed as a ligand, the polymerization system was also opaque and heterogeneous. A very broad PDI higher than 2 was acquired at low conversion. Moreover, the final product became gel, which is insoluble in common solvents such as THF, acetone and DMF, at an

Table 1
Effect of ligand on ATRP of TFEMA in cyclohexanone.^a

Entry	Ligand	[M] ₀ /[I] ₀ /[L]	[S]/[M] (v/v)	Time (h)	Conv ^b (%)	DP ^c A/B	M _n ^d (g/mol)	M _w /M _n ^e	Tacticity ^f mm/mr/rr (%)
1	PMDETA	135/1/1	1.3	6.5	81	109/153	25,850	1.54	-/-/-
2	PMDETA	270/1/1	2	5.5	74	200/276	46,510	1.45	18/32/50
3	PMDETA	135/1/1	1.3	4	56	76/129	21,520	1.40	-/-/-
4	PMDETA	270/1/1	1.3	6	80	216/304	51,220	1.53	31/28/41
5	bpy	53/1/1	2	3	87	46/66	11,230	1.24	32/26/42
6	bpy	107/1/1	2	4.5	80	86/109	18,460	1.28	-/-/-
7	bpy	133/1/2	1.2	5	75	100/136	22,990	1.11	-/-/-
8	bpy	267/1/2	2	5	77	206/213	35,930	1.18	27/27/46
9	bpy	400/1/2	3	2.5	52	208/281	47,350	1.26	26/24/50
10	bpy	400/1/2	3	5	62	248/326	54,910	1.29	-/-/-
11	Me ₆ TREN	313/1/2	2	3	8.0	25/-	-	-	11/37/52
12	Me ₆ TREN	313/1/2	3	5	21.3	67/1035	174,030	2.48	-/-/-
13	Me ₆ TREN	100/1/1	2	5	20	-	--	-	-/-/-
14	Me ₆ TREN	267/1/1	2	5	22	59/1005	168,980	3.22	-/-/-
15	Me ₆ TREN	200/1/1	2	7	Gel	-	-	-	21/30/49
16	Me ₆ TREN	267/1/1	2	10	Gel	-	-	-	-/-/-
17	Me ₆ TREN	267/1/1	2	10	Gel	-	-	-	-/-/-

^a The polymerization was carried out at 80 °C except for entries 1, 2, 3, 4, 5, which were all conducted at 70 °C.

^b Monomer conversion based on ¹H NMR method.

^c A – calculated from M_{TFEMA} × Conv_{NMR}, and B – evaluated with Eq. (1) from ¹H NMR.

^d Evaluated from ¹H NMR.

^e SEC results using PS as standard.

^f Calculated from the method reported by Okamoto et al. [59].

extending reaction time (as shown in entries 12–17). The activity of N-based ligands in ATRP is correlated with the number of coordinating sites as N₄ > N₃ > N₂ ≫ N₁ in the heterogeneous system [47]. In a heterogeneous system, Me₆TREN/Cu(I) complex would give more active propagating species with promoting propagating rate, which would lead to the breaking of the balance between the activation and deactivation in the ATRP process. In our experiments, when conducting polymerization of TFEMA with Me₆TREN as a ligand, a low deactivator concentration and a very fast activation would lead to an instant great increase in monomer radical concentration, which leads to a higher apparent rate constant (*k*_{app}) and high polydispersity. Generally, gel formation is easily observed in systems where significant transfer to polymer occurs, e.g., in acrylate polymerizations rather than methylacrylate polymerization due to steric hindrance induced by a substituent of the double bond. In the present system, high concentration of propagating radical transfer to ethyl in the side group of the polymer chain may possibly take responsibility for gel formation during TFEMA ATRP using Me₆TREN as a ligand.

To better understand the mechanism of ATRP, the stereochemistry of TFEMA polymerization was also investigated. The tacticity of PTFEMA is calculated from ¹H NMR of α-methyl group according to the signal assignments reported in the literature [59]. Indeed, as shown in Table 1, PTFEMA homopolymers prepared using present ATRP system have similar diad sequence composition to that prepared by conventional radical polymerization using AIBN or BPO initiator and within experimental error. This phenomenon has already been found by several other groups, as demonstrated for similar type of radical intermediate for ATRP as that for the conventional free radical polymerization [61].

3.3. Kinetic study

To seek deep insight into the reasons for the effect of ligand on ATRP of TFEMA, we further investigated the polymerization kinetics from ¹H NMR analysis in terms of the evolution of monomer conversion by monitoring variation of sum of the peak intensity for the double bond –CH_dCH₂ (5.85 and 6.19 ppm) protons from TFEMA to the sum of that for –CH₂–CF₃ from monomer at δ 4.49 ppm and polymer at δ 4.33 ppm. Intermittent sampling method was applied here to get samples for various analyses, such as ¹H NMR and SEC as detailed in the experimental

part. Fig. 5 shows the semilogarithmic kinetic plots for ATRP of TFEMA with [M]₀/[I]₀/[Cu(I)Br]₀/[L] of 100:1:1:2 for bpy system, and 100:1:1:1 for PMDETA system. For bpy system, after a few minutes, i.e. less than 6 min, the semilogarithmic kinetic plot is linear (dashed line in Fig. 5). This demonstrates that the polymerization rate is proportional to monomer concentration and indicates that the concentration of growing radicals is constant during the polymerization reactions after a few minutes [24,62].

It should be noted that the linear kinetic plot do not start in origin, which should be discussed in detail later. Indeed, Hvilsted group also found that the first-order plots for TFEMA ATRP using ethyl 2-bromoisobutyrate as an initiator and *N*-(*n*-propyl)-2-pyridylmethanimine (*n*-Pr-1) as a ligand at [M]₀: [I]₀: [CuBr]₀: [n-Pr-1] = 117:1:1:2 do not start at origin for temperature above 80 °C, i.e., 90 °C, 100 °C, and 110 °C [44]. We argue against the cause that they claimed for this phenomena resulted from the time needed to reach the required high temperature, since we found that kinetic plot is very similar to that for the polymerization that was performed with the reaction mixture heated at 80 °C for 10 min to

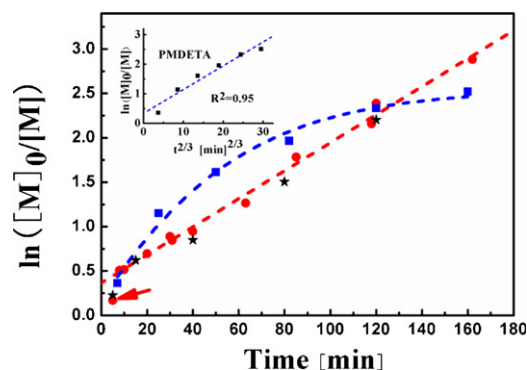


Fig. 5. Semilogarithmic kinetic plots for ATRP of TFEMA in cyclohexanone (cyclohexanone/monomer (v/v) = 1/1) at 80 °C using ligand of PMDETA (■), and bpy (●) with [M]₀/[I]₀/[Cu(I)Br]₀/[L] = 100/1/1/X (X = 1 for PMDETA and X = 2 for bpy), the dashed lines are only for the eyes. The five-star points represent the data from bpy system initial addition of CuBr₂ ([CuBr₂]₀/[CuBr]₀ = 1/9). Inset is ln([M]₀/[M]) vs. t^{2/3} for PMDETA system (in which the dashed line represents best linear fit for all the data with a correlation coefficient R² = 0.95).

Table 2
Polymerization phenomena of ATRP of TFEMA and solubility of CuBr (or CuBr₂)/ligand complex.

Catalyst system	Polymerization phenomena ^a	Solubility of ligand complex ^b	
		CuBr/ligand	CuBr ₂ /ligand
[bpy] ₀ /[CuBr] ₀ = 2/1	The reaction mixture after mixed is brown and transparent. Green precipitate presents after 10 min, and the whole reaction mixture becomes green and turbid	1/2 brown transparent (soluble)	1/2 green precipitation turbid (lightly soluble)
[PMDETA] ₀ /[CuBr] ₀ = 1/1	The reaction mixture after mixed turns from transparent and light green to cloudy and green right away, and then whole reaction mixture successively becomes dark green and opaque	1/1 Green transparent (soluble)	1/1 blue semitransparent (partially soluble)
[Me ₆ TREN] ₀ /[CuBr] ₀ = 1/1	The reaction mixture after mixed is opaque, and the whole reaction mixture gradually becomes transparent with little yellow	1/1 colorless soluble	1/1 golden partially soluble
[bpy] ₀ /[CuBr] ₀ /[CuBr ₂] ₀ = 2/0.9/0.1	The reaction mixture after mixed is brown and opaque, green precipitate presents after 6 min, and the whole reaction mixture becomes green and turbid	–	–

^a ATRP of TFEMA using different ligands in cyclohexanone (cyclohexanone/monomer, v/v = 1/1) at 80 °C.

^b CuBr (or CuBr₂)/ligand complex is dispersed in cyclohexanone/monomer (v/v = 1) with [monomer]/[CuBr (or CuBr₂)] = 100/1, the solubility and color are observed in a sealed flask free of oxygen.

reach equilibrium before the addition of MEBriB to initiate the polymerization (defined $t = 0$ when MEBriB was added).

However, for PMDETA system as shown in Fig. 5, the curved plot demonstrates that the radical concentration is continuously decreased during the polymerization reactions because of continuous consumption of monomer, irreversible termination of radical–radical coupling or a side reaction involving a radical transfer from the propagating chain to the ligand species to form nonpropagatable (dead) chains, as has been proposed by other research groups [63,64].

There were two main kinetic descriptions of the conversion vs. time, one is proposed by Matyjaszewski et al. [48,57], which is based on a constant radical concentration due to the equilibrium between polymer radicals, dormant chains and copper species (Eq. (2), denoted as M-equ.), while the other one developed by Fischer et al., [65,66] is based on the persistent radical effect (Eq. (3), denoted as F-equ.)

$$\ln \frac{[M]_0}{[M]} = k_p K_{eq} \frac{[RX]_0 [Cu^I]_0}{[Cu^{II}]_0} t = K_{Matyjaszewski} t \quad (2)$$

$$\ln \frac{[M]_0}{[M]} = \frac{3}{2} k_p ([RX]_0 [Cu^I]_0)^{1/3} \left(\frac{K_{eq}}{3k_t} \right)^{1/3} t^{2/3} = K_{Fischer} t \quad (3)$$

As the kinetic plots shown in Fig. 5, Eq. (2) can apply in bpy system, indicating that, after a few minutes, the atom transfer equilibrium constant ($K_{eq} = k_a/k_d$) and/or the Cu^I and/or initiator concentrations are sufficiently low and the Cu^{II} concentration is sufficiently high [67,68]. However, inset in Fig. 5 is $\ln([M]_0/[M])$ vs. $t^{2/3}$ for PMDETA system, the plot is linear suggesting that the data is well fitted with Eq. (3), which means that after a very short time $[Cu^{II}] \gg [R^*]$. In this case the radical concentration is controlled by the concentration of the activator, deactivator and ‘dormant’ chains and from that point onwards all reactant concentrations can be effectively calculated in time, and during the polymerization the concentrations of both RX and Cu^I are continuously decreasing, resulting in a decrease of the polymerization rate [65,66].

The slopes of F-equ and M-equ kinetic plots yielded the apparent rate coefficients of $15.2 \times 10^{-4} \text{ s}^{-1}$ and $2.7 \times 10^{-4} \text{ s}^{-1}$ for PMDETA and bpy systems, respectively. These are in reasonable agreement with the values of $1.6 \times 10^{-4} \text{ s}^{-1}$ to $2.9 \times 10^{-4} \text{ s}^{-1}$ reported for ATRP of TFEMA using ethyl 2-bromoisobutyrate as initiator and *N*-(*n*-propyl)-2-pyridylmethanimine (*n*-Pr-1) as ligand at $[M]_0:[I]_0:[CuBr]:[n\text{-Pr-1}] = 117:1:1:2$ at 80–110 °C [44].

So far, there have been a few reports on the kinetics of fluorinated (meth)acrylates in free radical polymerizations as well as in RAFT or ATRP. For monomers of type $\text{CH}_2=\text{CHCOO}-(\text{CH}_2)_n-\text{C}_m\text{F}_{2m+1}$, it was demonstrated that n has a significant influence on

the reactivity of the monomer compared with *m*. However, the conclusions are quite different from those of different research groups. For example, Ameduri et al. reported that polymerizations of fluorinated (meth)acrylates proceed rather slowly compared to nonfluorinated monomers [69], on the contrary, Beuermann et al. declared that the propagation rate coefficient (k_p) for the fluorinated monomer is higher than that of corresponding nonfluorinated methacrylate monomer at identical temperature, possibly because of less interactions between the macroradicals compared to nonfluorinated systems [70]. Our finding is consistent with the results from Beuermann et al., since the apparent rate constants of MMA ATRP have previously been reported in the range of $(0.10\text{--}5) \times 10^{-4} \text{ s}^{-1}$, which is lower than that from present study [71].

As stated before, the activity of Cu^{II} and Cu^I/ligand depends dramatically on their solubility in the polymerization medium [24]. It is interesting to ask why the ATRP of TFEMA in these three ligand systems is heterogeneous but exhibits obvious controllability. To answer this, further evidence for the solubility of CuBr (or CuBr₂)/ligand complex is included in Table 2. It demonstrates that the polymerization was heterogeneous because CuBr₂/ligand (see mechanism illustrated in Fig. 6) was not very soluble in the polymerization media. In these systems, the deactivator dissolves poorly or precipitates out of the system during the reaction and as a consequence will show a ceiling Cu^{II} concentration [72,73].

For bpy system, possibly because of the insolubilization rate coefficients (k_{insol}) are higher than the solubilization rate coefficients (k_{sol} , Fig. 6), an equilibrium concentration of copper species will be reached only after a few minutes, judging by the color change during the polymerization after mixing all the reactants, and by similar polymerization phenomena for the bpy system with initial addition of CuBr₂ ($[CuBr_2]_0/[CuBr]_0 = 1/9$) to that with only CuBr (Table 2). This is also demonstrated by the fact that the kinetic plot is almost the same for bpy system without addition of CuBr₂ to that for bpy system with initial addition of CuBr₂ ($[CuBr_2]_0/[CuBr]_0 = 1/9$). Two conclusions might be drawn. Firstly, the initial Cu^{II} concentration before the addition of initiator

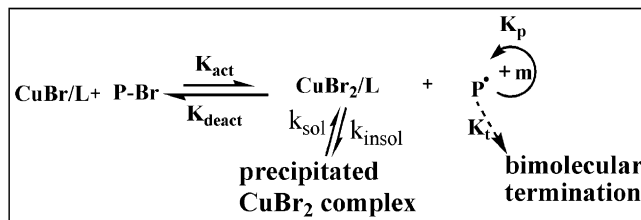


Fig. 6. Schematic illustration for heterogeneous ATRP mechanism of TFEMA.

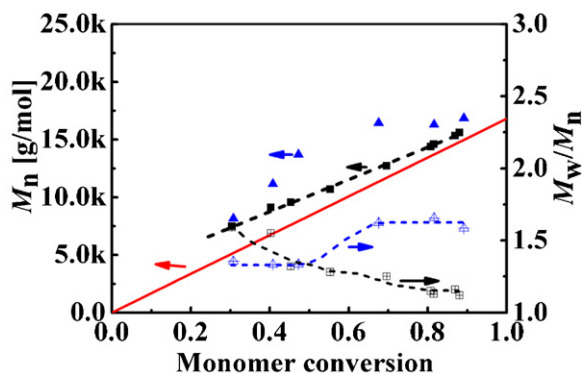


Fig. 7. The dependence of molecular weight, M_n (as evaluated from $^1\text{H NMR}$), and molecular weight polydispersity (M_w/M_n) upon monomer conversion for ATRP of TFEMA at 80°C with various ligands of PMDETA (\blacktriangle), and bpy (\blacksquare) (the straight line represents the theoretical molecular weight at certain monomer conversion, the dotted curves are only for the eyes).

is lower than the equilibrium value. Although the Cu^{I} concentration is relatively high, owing to the higher oxidation potential of the bpy complexed metal center than that of PMDETA or Me_6TREN complexed metal center, leading to a greater tendency toward radical deactivation and lower overall concentration of radical species. A lower irreversible termination is noted in the initial stage of the polymerization [28–30]. In other words, after a few minutes, the dissolved Cu^{II} is constant and high enough to minimize termination events, as a result a controlled polymerization with a low fraction of dead polymer chains is expected. Secondly, the initially added solid CuBr_2 does not dissolve well [74] and as a result will not contribute to the control of the polymerization leading to a similar kinetic plot to that without CuBr_2 . However, for PMDETA or Me_6TREN system, although the solubilization coefficients (k_{sol}) are high enough judging by the fast change of color after mixing all the reactants, the deactivation rate of growing TFEMA chains is not fast enough in comparison with PFEMA propagation. These are due to the electronic properties of these two ligands. This combination results in bad or even loss of control on TFEMA ATRP.

Fig. 7 shows the dependence of number average molecular, $M_{n,\text{NMR}}$ (as evaluated from $^1\text{H NMR}$), and polydispersity (M_w/M_n) vs. conversion for ATRP of TFEMA with PMDETA and bpy as ligand, the straight line in the plot represents the theoretical molecular weight at certain monomer conversion. For bpy system, the M_n evolves linearly with conversion, and measured values of M_n are very close to the theoretical prediction based upon $([\text{M}]_0 - [\text{M}]_t)/[\text{In}]_0$ under the reaction conditions used here. Moreover, an initiator efficiency derived from $M_{n,\text{NMR}}/M_{\text{theoretical}}$ is from 68% for 30% of monomer conversion to 95% for 88% of monomer conversion, indicating slow initiating but a high initiator efficiency, and thus small contribution of irreversible transfer, further

supporting a living process of TFEMA polymerization initiated with bpy system [52].

The polydispersities for all the PTFEMA obtained by ATRP using bpy as ligand are relatively low and decrease with conversion and increasing chain length, i.e., reaching value of ca. 1.1 at about 80% conversion. At the early stage of the reaction, the polymerization system had a higher initial Cu^{I} concentration and low amount of dissolved Cu^{II} /ligand complex due to low solubilization coefficients (k_{sol}). This resulted in a high radical flux and therefore a high termination rate. Irreversible radical termination can cause a decrease in initiation efficiency and high PDI. After the initial period the reaction rate decreases and so does the termination rate, and at higher conversions the polydispersity indices decrease [75].

However, for PMDETA system, it shows that although the M_n increases linearly with conversion, the measured values of M_n deviates from the theoretical prediction significantly under the reaction conditions used here. This may be due to slow exchange reactions which result in low initiation efficiencies and the termination by radical-radical coupling. The polydispersity indices M_w/M_n were relatively broad (more than 1.40) that may be because of a gradual loss of reactive species resulting from irreversible termination which can be seen in the first-order plot. Moreover, on the contrary to that from bpy system, the polydispersities for all the PTFEMA increase with conversion and increasing chain length, suggesting that the chain transfer may become increasingly significant with the increase of molecular weights for PMDETA system [75]. All these further demonstrate that the PMDETA-based system provides the undesirable characteristics of low initiation efficiency, high polydispersity, and uncontrollable apparent polymerization rate, and thus bad control over polymerization process.

3.4. Chain extension

To further figure out the effect of ligand, PTFEMA-Br derived from ligand bpy or PMDETA was employed as macroinitiator for block copolymerization with HEMA-tms, to confirm the “living” chain end of the polymer (Fig. 8).

Table 3 lists the data for the chains extension reaction using the two macroinitiators, PTFEMA-Br with similar molecular weight (M_n) derived from bpy system and PMDETA system, respectively. The chain extension reactions were both carried out in acetonitrile at 70°C with $[\text{HEMA-tms}]_0/[\text{PTFEMA-Br}]_0/[\text{CuCl}]_0/[\text{bpy}]_0 = 40/1/1/2$.

The conversion of HEMA-tms reached about 89% as evaluated from $^1\text{H NMR}$ after 23 h using PTFEMA-Br as a macroinitiator from bpy system, indicating a high initiating efficiency of the initiator. The SEC curve of the resultant block copolymer shifts toward high molecular weight, and is symmetric and unimodal (Fig. 9a). The successful extension of the well-defined PHEMA-tms block further demonstrates “living” character of the macroinitiator and well-controlled ATRP of TFEMA using bpy as ligand. On the contrary, the conversion of HEMA-tms came to only about 41% after 23 h using

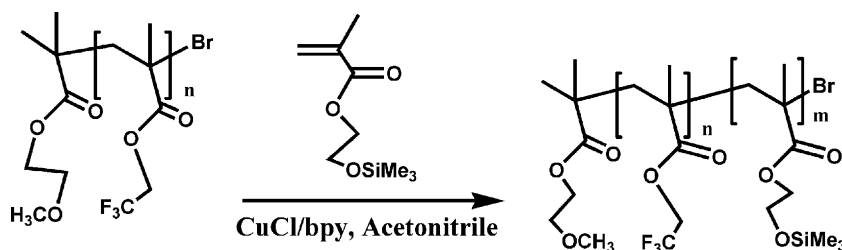


Fig. 8. Chain extension from ATRP using PTFEMA-Br as macroinitiator.

Table 3
Chain extension using PTFEMA-Br as macroinitiator.^a

Entry	Macroinitiator		Block copolymer	
	M_n^b (g/mol)	M_w/M_n^c	Monomer conversion ^b (%)	M_w/M_n^c
1	11,100	1.26	89	1.27
2	10,800	1.62	41	2.12

^a Reaction condition: [HEMA-tms]₀/[PTFEMA-Br]₀/[CuCl]₀/[bpy]₀ = 40/1/1/2 at 70 °C, reaction time = 23 h, the macroinitiator PTFEMA-Br in entries 1 and 2 was prepared using bpy and PMDETA as ligand, respectively.

^b Evaluated from ¹H NMR.

^c SEC performed using THF as eluent and narrow dispersed polystyrene as standard.

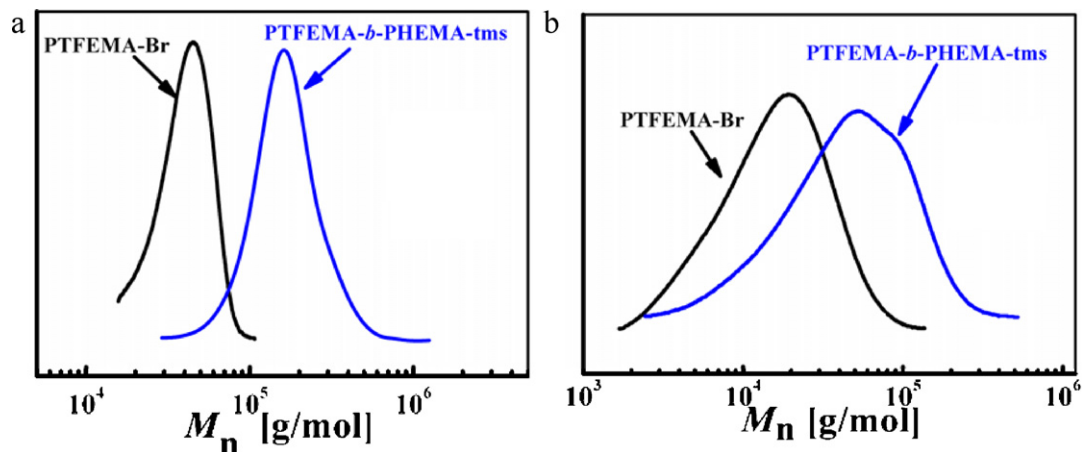


Fig. 9. SEC curves of (a) macroinitiator derived from ATRP of TFEMA using bpy as ligand and PTFEMA-*b*-PHEMA-tms from the macroinitiator, and (b) macroinitiator derived from ATRP of TFEMA using PMDETA as ligand and PTFEMA-*b*-PHEMA-tms from the macroinitiator.

Table 4
Bulk properties of the prepared polymer.

Entry	M_n (NMR) (g/mol)	M_w/M_n (SEC)	T_g (DSC) (°C)	Thermo-stability (TGA)			Static contact angle (°)
				T_{SWL} (°C)	T_{10WL} (°C)	WL ₃₀₀ (%)	
1	11,090	1.21	48	108	213	69	82 ± 2
2	25,370	1.11	65	131	213	64	85 ± 2
3	38,800	1.18	74	162	238	37	98 ± 3
4	51,240	1.29	75	168	246	29	96 ± 2

PTFEMA-Br as macroinitiator from PMDETA system. The low initiating efficiency for PTFEMA-Br derived from PMDETA system further suggests that the loss of Br and chain transfer occurred during the polymerization of TFEMA [52,76]. Fig. 9b shows SEC curves of macroinitiator derived from ATRP of TFEMA using PMDETA as ligand and PTFEMA-*b*-PHEMA-tms from this macroinitiator. The SEC curve of the resultant block copolymer is not only broad but also asymmetric, further demonstrating bad-controlled ATRP of TFEMA using PMDETA as ligand.

3.5. Bulk properties of the homopolymer PTFEMA

We also examined the bulk properties such as, glass transition temperature, thermo-stability, and film hydrophobicity of the PTFEMA homopolymer with different molecular weights. Table 3 lists the data of PTFEMA with variation of number average molecular weight (M_n) Table 4.

The T_g of PTFEMA increases from 48 °C for the sample with M_n = 11,090 g/mol to about 75 °C for the sample with M_n = 51,240 g/mol. This is believed to be because of the fact that the mobility of chain segment decreased for samples with higher M_n . Above a critical M_n , T_g should no longer increase with the molecular weight. [59] It was reported that the PTFEMA with M_n = 8600 g/mol exhibits a T_g at 59 °C. [59] It was also reported

that a T_g of 74 °C with M_n = 384,000 g/mol and 78 °C with M_n = 574,000 g/mol for PTFEMA sample was due to differences of their syndiotacticity [44]. In fact, when T_g is plotted against $1/M_n$ (Fig. 10), an almost linear relationship is demonstrated ($R^2 = 0.98$), a maximum T_g of 82 °C is reasonably extrapolated from the fitted line.

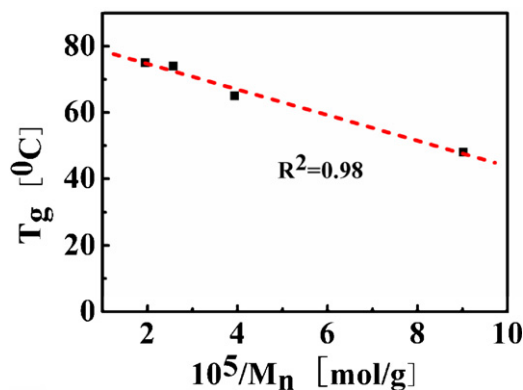


Fig. 10. The dependence of glass transition temperature of PTFEMA on the number average molecular weight (M_n).

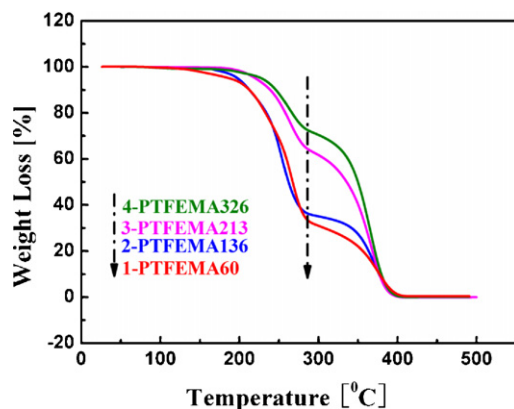


Fig. 11. TGA curves for PTFEMA samples with various molecular weights, the numbers 1–4 correspond to that in Table 4.

Fig. 11 shows thermo-stability profiles of the samples with different molecular weights as evaluated from the thermogravimetric analysis (TGA), and some of the data are included in Table 3. A two-stage degradation behavior with two distinctive plateaus for all the samples is observed which is in good agreement with the observation by other researchers [41,44]. The starting temperature for weight loss (T_{SWL}) significantly increases with the increase of the molecular weight (M_n), for example, $T_{SWL} = 108^\circ\text{C}$ increases to 168°C as the $M_n = 11,090$ g/mol increases to $51,240$ g/mol, moreover, the temperature for 10% weight loss ($T_{10\%WL}$) is at 213°C , 213°C , 238°C , and 246°C for PTFEMA sample with $M_n = 11,090$, $25,370$, $38,800$, and $51,240$ g/mol, respectively. These indicate that the sample with higher molecular weight is more stable compared to that with lower molecular weight. The weight loss at 300°C (WL_{300}), which is almost corresponding to the temperature for the beginning of the second plateau in the TGA profiles of all the samples (Fig. 9), decreases ranging from 69% to 28% as the molecular weight increases from $11,090$ to $51,240$ g/mol, since the content for $-\text{CF}_3$, $-\text{CH}_2\text{CF}_3$, $-\text{OCH}_2\text{CF}_3$, and $-\text{COOCH}_2\text{CF}_3$ in the polymer chain is around 40, 49, 58, and 75%, respectively. This suggests that the degradation behavior remarkably depends on the molecular weight of PTFEMA, for example, for sample with low molecular weight ($M_n = 11,090$, and $25,370$ g/mol), the weight loss routes for first plateau might be ascribed from bond cleavage either in the ester group (between the carbonyl and oxygen), between the ester group and the fluorinated ethyl, or in the ethyl pendant chain [44], and degradation of main chain, while the second plateau is mainly from the degradation of main chain, for sample with high molecular weight ($M_n = 38,800$, and $51,240$ g/mol), however, the weight loss (less than 37%) for first plateau might be mainly ascribed from the loss of $-\text{CF}_3$, and the second plateau derives from the cleavage of part of the side chain and degradation of main chain. The detailed thermo-degradation mechanism depends on further study, such as FTIR–TG and TG–MS and will be reported in another paper.

Homopolymer solutions in THF at 0.2 mg/mL with different M_n were dropped on a cleaned slide glass and dried at room temperature in a desiccator before water contact angle analysis. As shown in Table 3, the static contact angle of water on PTFEMA films are ranged in 82 – 98° . Moreover, it seems that film from lower molecular weight sample has lower contact angle of water than that from higher molecular weight sample, for example, the contact angle for film from sample with $M_n = 11,090$ g/mol is 82° , whereas that for film from sample with $M_n = 51,240$ g/mol is 96° (entries 1 and 4 in Table 3), which might be because of pronounced “end-group effect” for the sample with low molecular weight.

4. Conclusion

In summary, we have demonstrated that well-defined low-fluorinated homopolymer poly(trifluoroethyl methacrylate), PTFEMA, could be prepared by heterogeneous atom transfer radical polymerization (ATRP) using didentate amines, bpy as ligand in cyclohexanone in the presence of initiator methoxyl ethylene 2-bromoisobutyrate. The obtained PTFEMA has a number-average molecular weight (M_n) close to the calculated value and a relatively narrow polydispersity. The resulting homopolymer with high molecular weight shows higher thermo-stability.

Acknowledgements

We thank the Project of Leading Talent of Guangdong Province, the Outstanding Overseas Chinese Scholars Funds of the Chinese Academy of Sciences and NSF of China for financial support of this project. Dr. Ian Wyman is thanked for language polishing.

References

- [1] N.M.L. Hansen, K. Jankova, S. Hvilsted, *Eur. Polym. J.* 43 (2007) 255–293.
- [2] R.J. Plunkett, U.S. Patent 2, 230, 654 (1961).
- [3] J. Scheirs, *Modern Fluoropolymers*, Wiley, New York, 1997.
- [4] I.J. Park, S.B. Lee, C.K. Choi, *J. Appl. Polym. Sci.* 54 (1994) 1449–1454.
- [5] R.D. van de Grampel, *Surfaces of Fluorinated Polymer Systems*, Technische Universiteit Eindhoven, 2002.
- [6] G. Hougham, K. Johns, P.E. Cassidy, *Fluoropolymers: Synthesis and Properties*, Plenum, New York, 1999.
- [7] M. Morita, H. Ogisu, M. Kubo, *J. Appl. Polym. Sci.* 73 (1999) 1741–1749.
- [8] J.G. Riess, *Curr. Opin. Colloid Interface Sci.* 14 (2009) 294–304.
- [9] J. Eastoe, S. Gold, D.C. Steytler, *Langmuir* 22 (2006) 9832–9842.
- [10] Z. Zeng, B.S. Phillips, J.C. Xiao, J.M. Shreeve, *Chem. Mater.* 20 (2008) 2719–2726.
- [11] C. Huang, H.E. Katz, J.E. West, *Langmuir* 23 (2007) 13223–13231.
- [12] E.M.W. Tsang, Z.B. Zhang, A.C.C. Yang, Z.Q. Shi, T.J. Peckham, R. Narimani, B.J. Frisken, S. Holdcroft, *Macromolecules* 42 (2009) 9467–9480.
- [13] J.E. Hensley, J.D. Way, *Chem. Mater.* 19 (2007) 4576–4584.
- [14] L.M. Tang, Y. Li, X.M. Wu, X.F. Shan, W.C. Wang, *Adv. Technol.* 15 (2004) 39–42.
- [15] T. Imae, *Curr. Opin. Colloid Interface Sci.* 8 (2003) 307–314.
- [16] S.J. McLain, B.B. Sauer, L.E. Firment, *Macromolecules* 29 (1996) 8211–8219.
- [17] K. Tadano, Y. Tanaka, T. Shimizu, S. Yano, *Macromolecules* 32 (1999) 1651–1660.
- [18] M. Eberhardt, R. Mruk, R. Zentel, P. Théato, *Eur. Polym. J.* 41 (2005) 1569–1575.
- [19] (a) O.W. Webster, *Science* 251 (1991) 887;
- (b) Q.H. Zhang, X.L. Zhan, F.Q. Che, *J. Appl. Polym. Sci.* 104 (2007) 641–647.
- [20] G. Moad, E. Rizzardo, S.H. Thang, *Acc. Chem. Res.* 41 (2008) 1133–1142.
- [21] P.B. Zetterlund, Y. Kagawa, M. Okubo, *Chem. Rev.* 108 (2008) 3747–3794.
- [22] (a) B. Ameduri, B. Boutevin, *Well Architected Fluoropolymers: Synthesis Properties and Applications*, Elsevier, Amsterdam, 2004;
- (b) P. Lacroix-Desmazes, B. Ameduri, B. Boutevin, *Collect. Czech. Chem. Commun.* 67 (2002) 1383–2141;
- (c) B. Ameduri, *Macromolecules* 43 (2010) 10163–10184.
- [23] (a) D. Yang, L. Tong, Y.J. Li, J.H. Hu, S. Zhang, X.Y. Huang, *Polymer* 51 (2010) 1752–1760;
- (b) Y.J. Li, S. Zhang, H. Liu, Q.N. Li, W.X. Li, X.Y. Huang, *J. Polym. Sci. Polym. Chem.* 48 (2010) 5419–5429;
- (c) L. Tong, Z. Shen, D. Yang, S. Chen, Y.J. Li, J.H. Hu, G.L. Lu, X.Y. Huang, *Polymer* 50 (2009) 2341–2352;
- (d) Y.J. Li, S. Chen, S. Zhang, Q.N. Li, G.L. Lu, W.X. Li, H. Liu, X.Y. Huang, *Polymer* 50 (2009) 5192–5199.
- [24] (a) J.H. Xia, K. Matyjaszewski, *Chem. Rev.* 101 (2001) 2921–2990;
- (b) N.V. Tsarevsky, K. Matyjaszewski, *Chem. Rev.* 107 (2007) 2270–2299;
- (c) A.P. Narainen, S. Pascual, D.M. Haddleton, *J. Polym. Sci. Part A: Polym. Chem.* 40 (2002) 439–450.
- [25] (a) M. Kato, M. Kamigaito, M. Sawamoto, T. Higashimura, *Macromolecules* 28 (1995) 1721–1723;
- (b) J.S. Wang, K. Matyjaszewski, *J. Am. Chem. Soc.* 117 (1995) 5614–5615.
- [26] (a) M.H. Acar, N. Bicak, *J. Polym. Sci. Part A: Polym. Chem.* 41 (2003) 1677–1680;
- (b) A. Mittal, S. Sivaram, *J. Polym. Sci. Part A: Polym. Chem.* 43 (2005) 4996–5008.
- [27] J. Xia, X. Zhang, K. Matyjaszewski, *ACS Symposium Series 760*, American Chemical Society, Washington, DC, 2000, p. 207.
- [28] J. Qiu, K. Matyjaszewski, L. Thouin, C. Amatore, *Macromol. Chem. Phys.* 200 (2001) 1625–1631.
- [29] R. Venkatesh, S. Harrison, D.M. Haddleton, B. Klumperman, *Macromolecules* 37 (2004) 4406–4416.
- [30] R.K. O'Reilly, V.C. Gibson, A.J.P. White, D. Williams, *J. Polym. Sci. Part A: Polym. Chem.* 42 (2004) 2921–2928.
- [31] W. Tang, N.V. Tsarevsky, K. Matyjaszewski, *J. Am. Chem. Soc.* 128 (2006) 1598–1604.
- [32] A. Hirao, K. Sugiyama, H. Yokoyama, *Prog. Polym. Sci.* 32 (2007) 1393–1438.

- [33] (a) A. Tuteja, W. Choi, M.L. Ma, J.M. Mabry, S.A. Mazzella, G.C. Rutledge, G.H. McKinley, R.E. Cohen, *Science* 318 (2007) 1618–1622;
(b) M. Lazzari, M. Aglietto, V. Castelvetro, O. Chiantore, *Polym. Degrad. Stabil.* 79 (2003) 345–351.
- [34] S.A. Brewer, C.R. Willis, *Appl. Surf. Sci.* 254 (2008) 6450–6454.
- [35] Z.J. Wei, W.L. Liu, D. Tian, C.L. Xiao, X.Q. Wang, *Appl. Surf. Sci.* 210 (2010) 3972–3976.
- [36] J.G. Riess, M.P. Krafft, in: R.M. Winslow (Ed.), *Blood substitutes*, Elsevier, 2006 (Chapter 24).
- [37] M.G. Dhara, S. Banerjee, *Prog. Polym. Sci.* 35 (2010) 1022–1077.
- [38] S.D. Personick, *Fiber Optic Technology and Applications*, Plenum Press, New York, 1985 (Chapter 2).
- [39] L. Yi, X. Zhan, F. Chen, L. Huang, F. Du, *J. Polym. Sci. Part A: Polym. Chem.* 43 (2005) 4431–4438.
- [40] J. Roussel, B. Boutevin, *J. Fluorine Chem.* 108 (2001) 37–45.
- [41] X.Y. Liu, J. Chen, P. Sun, Z.W. Liu, Z.T. Liu, *React. Funct. Polym.* 70 (2010) 972–979.
- [42] T.Y. Guo, D. Tang, M. Song, B. Zhang, *J. Polym. Sci. Part A: Polym. Chem.* 45 (2007) 5067–5075.
- [43] S. Perrier, S.G. Jackson, D.M. Haddleton, B. Ameduri, B. Boutevin, *Macromolecules* 36 (2003) 9042–9049.
- [44] N.M.L. Hansen, M. Gerstenberg, D.M. Haddleton, S. Hvilsted, *J. Polym. Sci. Part A: Polym. Chem.* 46 (2008) 8097–8111.
- [45] L.F. Zhang, Z.P. Cheng, N.C. Zhou, R.M. Zhang, X.L. Zhu, *Macromol. Symp.* 261 (2008) 54–63.
- [46] H. Peng, I. Blakey, B. Dargaville, F. Rasoul, S. Rose, A.K. Whittaker, *Biomacromolecules* 10 (2009) 374–381.
- [47] W. Du, A.M. Nyström, Z. Lei, K.T. Powell, Y. Li, C. Cheng, S.A. Wickline, K.L. Wooley, *Biomacromolecules* 9 (2008) 2826–2833.
- [48] J.S. Wang, K. Matyjaszewski, *Macromolecules* 28 (1995) 7901–7910.
- [49] X.S. Wang, N. Luo, S.K. Ying, *J. Polym. Sci. Part A: Polym. Chem.* 37 (1999) 1255–1263.
- [50] J. Xia, K. Matyjaszewski, *Macromolecules* 30 (1997) 7697–7700.
- [51] R. Kroll, C. Eschbaumer, U.S. Schubert, M.R. Buchmeiser, K. Wurst, *Macromol. Chem. Phys.* 202 (2001) 645–653.
- [52] L. Feng, J.W. Hu, Z.L. Liu, F.B. Zhao, *Polymer* 48 (2007) 3616–3623.
- [53] J.W. Hu, G.J. Liu, G. Nijkang, *J. Am. Chem. Soc.* 130 (2008) 3236–3237.
- [54] T. Kakiuchi, M. Nakanishi, M. Senda, *Bull. Chem. Soc. Jpn.* 61 (1988) 1845–1851.
- [55] A.E. Acar, M.B. Yagci, L.J. Mathias, *Macromolecules* 33 (2000) 7700–7706.
- [56] Z.T. Liu, J.G. Chen, Z.W. Liu, J. Lu, *Macromolecules* 41 (2008) 6987–6992.
- [57] J.L. Wang, T. Grimaud, K. Matyjaszewski, *Macromolecules* 30 (1997) 6507–6512.
- [58] F.B. Zhao, Z.L. Liu, L. Feng, J.P. Sun, J.W. Hu, *J. Polym. Sci. Part B: Polym. Phys.* 47 (2009) 1345–1355.
- [59] W.H. Liu, K. Tang, Y.Z. Guo, Y. Koike, Y. Okamoto, *J. Fluorine Chem.* 123 (2003) 147–151.
- [60] K. Matyjaszewski, K. Davis, T. Patten, M. Wei, *Tetrahedron* 53 (1997) 15321–15329.
- [61] D.M. Haddleton, C.B. Jasieczek, M.J. Hannon, A.J. Shooter, *Macromolecules* 30 (1997) 2190–2193.
- [62] K.A. Davis, H. Paik, K. Matyjaszewski, *Macromolecules* 32 (1999) 1767–1776.
- [63] M. Bednarek, T. Biedron, P. Kubisa, *Macromol. Rapid Commun.* 20 (1999) 59–65.
- [64] R. Sharma, A. Goyal, J.M. Caruthers, Y.Y. Won, *Macromolecules* 39 (2006) 4680–4689.
- [65] H. Fischer, *Macromolecules* 30 (1997) 5666–5672.
- [66] H. Fischer, *J. Polym. Sci. Part A: Polym. Chem.* 37 (1999) 1885–1901.
- [67] T. Fukuda, A. Goto, K. Ohno, *Macromol. Rapid Commun.* 21 (2000) 151–165.
- [68] H. Zhang, B. Klumperman, W. Ming, H. Fischer, R. van der Linde, *Macromolecules* 34 (2001) 6169–6173.
- [69] B. Guyot, B. Ameduri, B. Boutevin, M. Melas, M. Viguier, A. Coller, *Macromol. Chem. Phys.* (199) (1998) 1879–1885.
- [70] R. Siegmann, S. Beuermann, *Macromolecules* (43) (2010) 3699–3704.
- [71] M.H. Acar, C.R. Becer, H.A. Ondur, S. Inceoglu, *Polym. Preprints* 46 (2005) 433–434.
- [72] D.A. Shipp, K. Matyjaszewski, *Macromolecules* 33 (2000) 1553–1559.
- [73] M.A.J. Schellekens, F. de Wit, B. Klumperman, *Macromolecules* 34 (2001) 7961–7966.
- [74] M. van der Sluis, B. Barboiu, N. Pesa, V. Percec, *Macromolecules* 31 (1998) 9409–9412.
- [75] K. Matyjaszewski, *J. Phys. Org. Chem.* 8 (1995) 197.
- [76] M. Bednarek, K. Jankova, S. Hvilsted, *J. Polym. Sci. Part A: Polym. Chem.* 45 (2007) 333–334.